CTEC3406 Fuzzy Logic & KBS

EV Fuzzy Charging System

Jordan Tyler Gray (P2540338)[1]

[1]De Montfort University

June 2, 2022

Abstract

This report covers the design, development, implementation, and refinement of a fuzzy inference system to regulate the optimum charging of a lithium-ion based battery pack within an electric vehicle, implementing such system using MATLAB's fuzzy logic toolbox. The system aims to use information and infrastructure already available to existing EV's to meet the goal of prolonging the battery's service life by reducing the rate of cell degradation by following optimum profiles for charging current and maintaining optimum temperatures. It finds that existing vehicles have similar systems, providing the control hardware required to regulate both temperature and charge current, both of which are found to be leading factors in battery degradation. Existing work is found to have been completed near this area, with generic cell charging systems suggesting viability towards this project's feasibility. A proof of concept system demonstrating the use of fuzzy logic in this type of control system is designed and implemented, beginning to realise that potential for a system of this type to exist - but it short in the formation of accurate inference calibration, failing to realise the potential in it's totality. Further development would be required to increase the accuracy of the system before it could be considered a viable commercial solution.

Keywords

Fuzzy Logic, Electric Vehicle, Charging, Control System, Inference

1 Introduction

Fuzzy logic is a logical paradigm which connotes an output classification from data that hints degrees of truth to input classifications. Where binary logic can represent an entity as being wholly a member of a classification or it's complement, fuzzy logic handles an entity who partially belongs to a class, and may belong to two or many classifications at the same time, all to different degrees (Novak et al. (1999)). This type of logic is not limited to crisp values, and is combined with having the ability to accept a multitude of inputs to provide a one or many outputs, opening potential for narrow AI style decision making. Contained within this paper is an attempt to utilise this paradigm in order to develop an inference system which can unite with the emerging Electric Vehicle market which, since 2012, has expanded to cover around 15% of the car market and forecast to approach 40% - 50% by 2030 (Lilly (2021), Walton et al. (2020)).

One of the most crucial factors defining success for production vehicles in this market is their batteries and ability to charge with longevity in mind. Vehicles which cannot reliably maintain a long lifespan will not be desired by consumers, and ultimately will fail. Combining this with the theoretical environmental impact of quickly depleting lithium-ion batteries, and shortening the life time of a car into this, and it's rather simple to see why EV

manufacturers should be aiming to design systems which care for the batteries their cars use, prolonging the lifespan of the cells by slowing the rate of degradation as much as possible.

The proposed system is driven by this desire to prolong longevity.

2 Literature review

Some fuzzy battery charge systems already exist, such as a Lead Acid charging system produced in 1992 LIANG & NG (1993). The system had "Good performance statistics", and provides hope for the implementation of the system proposed here. Where publicly available literature falls down, however, is in the specialised field of charging an electric vehicle. This is predictable, since this type of knowledge is industrial secrets that sways into the befit of the manufacturers. So whilst certain the prevalence to which fuzzy control systems are implemented in this precise area cannot be foretold, we can infer from previous implementations that similar systems focusing on charging exist with moderate success.

Taking a look at the existing market finds that Tesla, a leading American electric automotive production company, guarantees their cars to degrade no more than 30% of capacity lost in 8 years, or 100k - 150k miles (values variate dependant on the model), whichever comes first ((2017)). However, it seems that the true degradation is considerably lower. Fred Lambert reported for Eletrek that his Model X 90D had only diminished by 10.5% after more than 317k miles (Lambert (2020)).

"Tesla has historically been able to limit degradation to reasonable levels thanks to its robust battery management system." (Lambert (2020)) Rates of decay are linked to the conditions in which the battery is operated and stored. Specifically, under abusive temperature environments, and over-voltage & over current events. There's also significant influence as an affect of current. Since we're focusing on charging, discharge rates will be disregarded in this system. It seems the maintenance of inventory can be significantly aided by controlling the current whilst charging. (Ouyang et al. (2019))

It has been observed that cells cycled in extreme temperature environment degrade faster than equivalents at room-temperature (Ouyang et al. (2020)). Also observed, is that cells will heat as they charge - particularly at high current rates (David (2009)). Inferred from this, a healthier cell can be influenced by preventing the battery from entering a hot environment. Counter to this, we know the battery itself is exothermic, tending to heat itself whilst cycling, so the the battery must also be prevented from overheating itself. EV manufacturers manage this with an active cooling & heating solution, typically involving using coolants, heat pipes and similar (Dober (2020), Wang et al. (2015), Oh & Park (2014)). The exact methods are not of consideration here, but rather just the fact that modern EV's typically contain active temperature regulation systems. From this, we can collate the output of temperature control, and the complimenting input of battery temperature. Since the papers referred to here agree in monitoring the surface temperature of the cell, the input can assume that the value it's receiving is, too.

The NEC (1999) standard for charging levels defines three levels of charging, which are determined by the type of charger in use.

	Amps	Volts
Level 1	24	120
Level 2	32	240
Level 3	400	240 ~ 600

Table 1: NEC Standard Charging Levels

Electric Vehicle Charging Equipment Installation Guide (2020), Thomson (1999)

As of yet, the upper boundary remains undefined; Level 3 could mutate as DC fast charge technologies are developed further (Bower (2015)). For now, it'll be assumed that this absolute. This provides the limit of 400 amp absolute max, and three charge rate bands. These levels only define maximum charge currents; A true charge current may fall anywhere below it's limit. To simplify, these boundaries can be unified into kW.

EV batteries may be considered under the definition of a 'Thermostatically Controlled

load', where a thermostat type behaviour is used to regulate their temperature towards a set point by calling for heat or cooling. (2007)

3 System Overview

The problem discovered is that the holding capacities of batteries will degrade over time, and this effect is significantly negatively amplified by behaviours of cycling, the environment, and even by the side effect of of charging in the form of heat. An industry standard solution to this is to condition the pack's charging, through limiting the current throughout the charge cycle, along side preventing the battery from entering an extreme temperature environment. The system this paper will attempt to create will be an extension to those industry standard methods, acting as a controller to the pre-existing hardware, except with the implementation of fuzzy control logic. We'll get started by examining the the input and outputs, and defining preliminary values for their sets and memberships. These values will be based on the research, combined with some guesswork and arbitrary pattern creation, which is expected to end in an inaccurately controlled portrayal of the proposed system, which can then be mutated and refined through testing to produce the results expected.

3.1 FIS type

Before this, the type of inference system that will be used must briefly be considered since it will determine how the input, output, and rules are defined. In fuzzy logic, there are two main types of fuzziness: Type 1 and Type 2.

A Type 1 inference system handles fuzzy sets, and the degrees of memberships that come with them, where strength of membership is strongly defined through a membership function.

Type 2 inference extends this system by adding uncertainty surrounding the membership function (Karnik & Mendel (2001), Mendel et al. (2014)).

The prototype being created will use a type 1 system, since there is no requirement to infer uncertainty with memberships, based on the research. It seems appropriate that all input and outputs will have strongly defined sets and membership functions.

MATLAB supports two types of type 1 fuzzy inference system. Sugeno and Mandami. According to Mathworks, Sugeno system is more suited to mathematical analysis, and is more computationally efficient, however at the cost of being less intuitive to implement Mamdani & Assilian (1975). This system won't have focus on the those parts of the use case. Combining this with the requirement to learn and implement the system in a short time frame, we'll use Mandami. It's intuitive rule bases are far more valuable in getting the system operational to some degree over computational efficiency. Should this seek a wider spread and the need for optimisation arises, then the system could be retrofitted to a more efficient Sugeno system at some time in the future.

The architecture of the system will dictated by the mandami system that we'll be using to implement with, where we'll have one or many inputs, and one or many outputs. Each input and output will have a max and minimum value, and regions defined within the range which determine which values belong to which set, and to what degree. After which, both sides of this system are conjoined with behaviour defining rules.

Working backwards from the knowledge of what the system needs to control achieve it's goal, the outputs can be determined and strictly defined. From there, the information required to infer their values can be calculated, leading to the development of the system with this i/o around this FIS architecture.

From reviewing the literature in this area, it's known that for this system to be successful it must have the capacity to govern the charging current and the temperature of the battery.

3.2 The outputs

3.2.1 Charge current

To achieve the first, the charging rate will be controlled by supplying a kilowatt value to the charger. We'll define the range available as being from 0kW, or no charging, to 350Kw. 250

kW is presently the maximum Level 3 charging current used by Tesla (Database (2021)). However, since the upper boundary remains undefined by the Nation Electric Code, 100kW above the market is provided for future expansion is included. This output's sets will be based on the charging level standards, thus it will consist of three three sets collating level 1, 2, and 3 output value ranges.

According to the NEC standards the standard maximum continuous and current for the three levels are as follows :

	Continuous	Peak
Level 1	2.88	3.6
Level 2	7.2	9.6
Level 3	576	720

Table 2: Max Continuous Current (Kw)

Electric Vehicle Charging Equipment Installation Guide (2020)

Output 1 will be defined by preliminary set regions using these values, with trapezoidal regions where the shoulders are defined by the continuous current, and the feet by the peaks. The end of the range will be capped at 350 kW.

	lf	ls	rs	rf
Level 1	0	0	2.88	3.66
Level 2	2.88	3.66	7.2	9.6
Level 3	7.2	350	350	350

Table 3: Output 1

3.2.2 Active Temperature Conditioning

Secondly, it must be proficient at regulating the temperature by governing the active temperature conditioning equipment for the battery pack. Unlike the charging rate output, there is no industry wide standardisation outside of thermostatic control which can used as a base, thus every car will have it's own way of handling temperature management. This forces this output into being more abstract, requiring that it has non-absolute values. Rather, it will be modelled after thermostatic control solutions, whereby a thermostatic device will request for cooling and heating to different strengths based on distance from the set point. (Database (2021))

Following this implementation model, four temperature regions are defined to match temperature change requests to different strengths: rapid cool, cool, heat, and rapid heat, where cool and heat are regular calls for temperature manipulation, and the two rapid ranges are for more drastic measures, i.e to quickly bring the battery back from an extreme temperature to a more healthy one. The system will monitor the temperature of the battery, and change the severity of the temperature manipulation dependant on how far the battery's temperature is from ideal (which is defined in 3.3.1). We can arbitrarily define the value range between -10 and 10, and evenly split the range into the four trapezoidal membership regions, with 20% overlap.

Region	lf	ls	rs	rf
rapid cool	-10	-10	-6	-4
cool	-6	-4	-1	1
heat	-1	1	4	6
rapid heat	4	6	10	10

Table 4: Output 2

3.3 The inputs

The system will need to know information about the state of the battery pack, alongside the charging environment, to be successful at controlling these outputs.

3.3.1 Battery Temperature

First, the Active Temperature Conditioning (3.2.2). For the system to manage the temperature, it must know the temperature which the battery is currently measured to be. The literature covered have all focused on surface temperature of the cells when measuring as opposed to the internal temperature, so we can assume that the temperature being received by this input is that of the cell's surface. The source isn't particularly pertinent, but may have an effect on calibration under the additional assumption that an internal temperature would differ from that of a surface temperature whilst the cell is cycling.

The optimal temperature range for battery preservation is between 15°C and 30°C Agwu et al. (2018). This input will aim to keep the pack within this range by managing the active temperature managing equipment controlled by the output defined in 3.2.2. Batteries are known to heat whilst being charged David (2009), so during an overheat event we can further help the pack cool by reducing the charge current. The same behaviour rules will be implemented for low temperatures too, since it's less healthy for the cell to be charged outside of the ideal range Smith et al. (2015).

This is used to define a mid region called 'Ideal' where we'll aim to have the pack remain. It'll span across the 15-30°range where the apex (defining the most ideal temperature) is in the center of these values ($\frac{30-15}{2} + 15 =$ 22.5°C). To implement this, we can use a trimf. To finish this input, the 'ideal' region is surrounded with sets to indicate a 'High' temperature, and a 'Low' temperature.

We'll account for any values lower than the 'low' overlap to be a part of the 'low' set, and the same for the 'high' set. To achieve this, we desire to use a Z-Shaped Membership Function (zmf) to define the fuzzy region, with no definite end to the set. However, limitations to the zmf prevent this from being viable (4.2), so instead we'll use a trapezoid function extending farther than would ever be expected to be reached. For this reason, the regions will extend to +/- 100°'s, and overlap into the center of the 'ideal' tri, indicating that as the input strays from ideal it will belong to a 'high' or 'low' to some degree.

3.3.2 Max Charging Supply

The system will also need to know the maximum charging current that is available. This information is obtained from the EVSE (Electric Vehicle Supply Equipment) that is connected, and will limit the maximum charge rate that the system will attempt to charge at.

The ranges on this input will match that of output 1, being based off of the max charge currents.

	lf	ls	rs	rf
Level 1	0	0	2.88	3.66
Level 2	2.88	3.66	7.2	9.6
Level 3	7.2	350	350	350

Table 5: Input 3

3.3.3 State of charge

The charge rate will be conditioned based on the current charge level of the battery to match the optimum charging profile for lithium-ion cells (Khan & Choi (2018), Valle et al. (2011)). This profile is drawn as a 'trickle' charge (low current) from 0%-10% of charge, followed by a plateau at the highest charge current to 50%. After which, the charge current declines linearly to 0 Kw as the battery fills to max.

Following this charge profile, an input can be drawn to accept the state-of-charge, that is the a percentage to which the battery is currently filled, which contains three regions to cover these stages of interest. Each will directly link to similar set on the output, determining the charge rate.

The first region, for trickle charging, will cover from 0% to 10%. Instead of transitioning immediately to the max charging rate, we'll ease the transition by declining this function at 8%, and begin gradually transitioning to the max rate. This new set needs to be reached in it's entirely at some point soon after 10%, but aiming to give a few percent's time to transition we'll define it to be reached at 15%.

This leads us into the 'Max speed' charging region, which will match this transition period by linearly grading from 8% to 15%, and remaining so until nearing 50% charge. Here, we'll use the right foot to define the linear decline; Starting at 50% and ranging to 100%, this region will decline it's membership. The hope here is that we can avoid adding another region to the system to perform the same functionality, however a complimenting region linked to a low charge speed may be required to get the desired behaviour. This will have to be determined during testing.

	lf	ls	rs	rf
Trickle	0	0	8	10
Max	8	15	50	100

Table 6: Input 6

3.3.4 Hardware Faults

For safety, we'll also take two non-fuzzy binary inputs, that notify our system when a fault condition is detected. How these faults are detected are not of concern, and we'll assume that they are accurate to the state of the equipment. The first is for a major fault, which we'll define as a serious problem event that indicates that the battery should not be charged due to some critical failure in the charger, the battery pack, the cooling system, or similar crucial equipment. When this input is high, there will be no output current.

Secondly, a minor fault. This indicates a non-critical failure that should limit the charging rate, but not outright prevent it. For example, this could indicate a some hardware is not performing optimally & requires service, but that it's still operational. When this input is high, the output will be limited to level 1 charge speeds.

For both of these values we can define a range reminiscent of analog binary, where the value can be between 0-1, anything less than half is considered 'low', and anything higher is 'high'. These inputs will have no overlap and be one sided. A stepper function would be the most ideal for this, specifically the Z-shaped membership function - however, limits within the system make this seemingly impossible to define so as a compromise, the regions will be drawn with trapezoidal functions where their shoulders and feet match exactly.

	lf	ls	rs	rf
High	0	0	0.5	0.5
Low	0.5	0.5	1	1

Table 7: Input 1 & 2

3.3.5 Battery Health

For future expansion, the system will also accept an input for the current health of the battery, in percentage of factory capacity inventory retained, where 100% represents a new battery that has not degraded, %70 represents a battery that can only hold %70 of it's factory equivalent capacity (the level that Tesla guarantees their batteries to) and 0% represents a battery that will not hold any charge. This way, if future research into suggests that charging behaviour should be altered at different levels of degradation to further prolong the batteries lifetime, the system may easily be modified to accommodate.

This input will have less care invested in it's sets, with entire speculatory regions.

	lf	ls	rs	rf
Unusable	0	0	10	25
Poor	10	25	30	35
Good	30	35	80	85
Exellent	80	85	100	100

Table 8: Input 4

3.4 The rules

Now that the ground work for the proposed system's architecture is laid out, one a final look over all of the inputs and their effect on the output will define the rules that define the final behaviour of the system.

3.4.1 Temperature

As discussed in 3.3.1, the known temperature of the battery will influence both 3.2.1's charging rate and 3.2.2's temperature control.

Set	Suggests 3.2.1
Low	Low charging
Ideal	No effect
High	Low charging
Set	**Suggests 3.2.2**
Low	Heating
Ideal	No effect
High	Cooling

3.4.2 Available Charging Current, & State of charge

Since these rules are tightly related, they'll be combined. The available charge current will

contribute a base of the rules defined here, the system will have a set of rules for every available charge level. This base will then be modified by the state of charge. Giving us 3^2 rules governing the charging output speed.

Set	Suggests 3.2.1
Trickle	Low charging
Max	Max available charging
Decline	Inversed max charge current.

Implemented, this creates rules resemble 15

3.4.3 Hardware faults

To implement, the requirement for a major fault will be a be a dependency for all other rules - not in-dependant rules. This will prevent them from firing and providing an output current, as is desired.

Separate rules matching the charge rules with minor high will exist, replacing the normal charging rules when minor is high with a low output.

At this stage, the implemented rule base contains 19 rules (4).

4 Testing

Immediately after implementing the system based on the design, testing was required to finalise the configuration to give the most accurate results. To achieve this, the script was modified in order to read test data from an excel workbook, evaluating the system with data present in a the spreadsheet and writing back all the results for analysis.

4.1 Defuzzification method

The results the system provides are determined by the defuzzification method (Mathwords (2021)). The script was modified further to cycle through all 5 defuzzification methods (Lom, Mom, Som, Bisector, and Centroid), repeating all the test evaluations for every method. 16

Analysing the results in 17, it was clear to see that Lom, Mom, and Som defuzzification methods were the least accurate for Output 1. These three types have been grouped, based on their wildly different results in comparison to centroid and bisector. The values varied significantly from the values expected. Generally for these three types, output 1 remained incredibly small as the available current rose and rules suggested a higher and higher output. Struggling to get above zero, or a trickle charge, for $\frac{40}{61}$ tests. The remaining test values would behave in a polar opposite fashion, where the output 1 would jump towards a significantly higher value than is reasonably expected. See row 40 in 17, where the max input is 50 kW, and the battery is at 80% suggesting that it should only be using some fraction of the 50 kW, yet the output was 360 kW for lom and 222.5 kW for som.

These same methods seemed to produce accurate results for Output 2, however. At the ideal 22.7°C, there was no or very little temperature conditioning call, and as the temperature rose, output 2 fell. The complimentary behaviour can also be observed. This is exactly the expected behaviour of the system. Time was not spent investigating further into why these methods were to producing such inaccurate results for output 1. Instead, they were written of as unsuitable for this use case, and attention was turned towards Centre and Bisector which appeared to behave closer to desired.

Examining one case from 16 (rows 47-51), the maximum input is 250 kW and the charge level of the battery increases through these tests, as if the pack was being charged :

Battery percentage	Centroid	Bisector
10	197.36	230.40
25	238.45	273.60
40	238.45	273.60
80	214.40	252.00
100	20.27	21.60

The results in this case are reminiscent of the others in this sheet, who display similar behaviour curves and inaccuracies, thus they won't be examined in detail here.

As determined in 3.3.3, the output is expected to start low, rise to max, then gradually fall towards 0 again as the battery approaches

100%. The results of this case show the output starting very high compared to the desired 'trickle' (0-10kW) charge desired in both methods, at 197.36 kW in centroid and worse at 230 kW in bisector. It rises as the battery enters the 'max' region, as expected. Peaking at 238.45 & 273.60 kW, and falling to around 20 kW at it reaches full. Whilst the evaluation shows the expected behaviour to a degree, it displays multiple issues with the values not being as expected in both inferences :

- The 'trickle' range at 10% should be considerably lower than the values observed, in the 0-10 kW range. This 'super slow' region is a crucial behaviour to prolonging longevity, yet the system over shoots by far.
- The 'Max' value at 25% and 40% should not exceed the 250 kW available. The available should govern as a limit and none of the output values should surpass it, however both
- 80% battery perfentage falls around half way between the 'max' region and 0 ; The expected output should be around half-way between the values found at 50% (Which is wholly max) and 100% (which is wholly 0). but remains around $\frac{214.40-\frac{238.45+20.27}{2}}{214.40} = 84.3306\%$ higher for centroid, and $\frac{252.00-\frac{273.60+21.60}{2}}{252.00} = 70.7317\%$ higher for bisector.
- The battery is still being charged at around double the 'trickle' current when it's 100% full. At 100%, the output should be 0 kW since the capacity it entirely saturated.

Comparing Center to Bisector in this same case, the first value is seen to be marginally closer to the desired 'trickle' range in centroid. The final value, which should be zero, matches also - being mildly closer to zero. The desired value to be found at 25% and 50% battery percentage should meet the max charge rates, which were 250 kW. Centroid was $250 - 238.45 = 11.55$ kW away, whilst Bisector was $273.60 - 250 = 23.60$ kW away - thus once more centered proved to be more accurate.

For this reason, the final system script defaults to the centroidal defuzzification method. Whilst it's results are still not particularly accurate, they're the most accurate in the current state of the system given the test data, and compared to the others that defuzzification methodologies that are available to the system.

4.2 ZMF could not produce the desired membership

In the membership definitions, it was assumed that a z-shaped membership function could be reversed, such that the 'slant' could face either direction on the scale. Some functions were defined this way, under this assumption. However, whilst attempting to implement, it quickly became clear that the Z-Shaped membership function did not seem to co-operate in this fashion, and would produce strange membership regions when attempting to reverse them. Instead, a compromise was made to change some of the memberships to trapezoidal, and use their shoulders to 'draw' the desired set membership. (10)

A significant difference between the zmf and trapezoidal, is the infinity to the bounds of the zmf; It extends to the full extent of the input range and beyond. The trapezoidal, however, is limited by the range between it's left and right sides. To account for this, the compromised memberships were extended farther than would be expected to be reasonably used, or to the end of the range.

4.3 Issues

4.3.1 Temperature charge bridging

A data sheet for testing 3.3.4 (11) sought to assert no charge was admitted if a major fault was reported. The sheet detected held data which should cover most combinations of sets being 'active', aiming to trigger as many cominations of rules as possible. Results in this sheet showed that in both Bisector and Centroid defuzzification methods, a low charge was being delivered; not the expected 0kW in some combinations. This indicated that some combination was triggering a rule which permit-

ted current to bridge through, when charging should be halted.

Investigating this further, the rule viewer was found to show why: rules 1, 4, & 7 hint to low output(12) for other conditions, with no regard to input 1. These rules correspond to current limiting rules that were intended to lower the output current by suggesting the lower output setting when a minor fault, or low charge rate was available. Since these rules used the 'or' operator to merge multiple conditions into a single rule, it was not possible to assert the major fault condition as with all the other rules, as this required the use of the 'and' operator. This means that even if major was high, minor being high would suggest low output current. This can likely be fixed by separating these rules into individuals that all assert the major fault is low using the 'and' operator.

Immediately, implementing this (2) change seemed to have had the desired result - the rule viewer showed the charge rate output drop to 0 when Major Fault was high, even when minor fault was high. Running the test again, all records dropped to zero except for the first. However, this seems to be some issue with the testing process, as manually entering the same values into the system gives the desired result (13).

4.3.2 Poor heat / cool performance

One observation that was made rather quickly whilst testing the system, was the poor performance of the heat/cool output. The arbitrary design of the output was poor: only three of the sets were made use of, 'Rapid cool', 'Cool' and 'heat'. 'Rapid Heat' was never used. Further, there was no neutral state for the output to fall to.

Implemented as designed (7), this output utilised the 'Rapid cool' when it actually desired 'cool', 'cool' was the neutral state. 'Heat' was the only set used as intended. This led to the output always low (3), calling for the system to cool the battery pack, when the battery was at the defined ideal temperature. It would also use dramatic cooling when the pack was not experiencing an temperature extreme. Further, there are only 3 input sets for temperature which leads to the impossibility to account for temperature extremes. Since the system does not have the sets to determine between a 'warm' and 'overheating' battery, there's no way for it to know when to activate the 'rapid' heat / cooling sets.

The solution revolves around re-designing the sets defining the i/o for temperature, and altering the rules to account for it. To start, we need some neutral state. Apposed to the idea of using a set to define this, the system was tested with only one rule influencing the output to observe where the output would fall naturally. The rule was fired to drift the output from resting before clearing it, and as desired the output returned directly to zero. This discovery tells us that the output can be re-created with no requirement to hint towards neutral. The output can instead have an empty region at 0 belonging to no set. Changing the rules to then utilise this, it should resolve the issue where the output was pulled low. For a set overhaul, we'll instead place a linear set both sides of this neutral zone, allowing the system to finely control the heal / cool calls from neutral to extreme as desired. This eradicates the need for the 'rapid' sets previously designed (8).

To make use of this new output, the temperature input will need to be modified also. Unlike the output, the input will will retain it's sets - however to get the linear control over the output desired, the memberships will need to be altered. Input 5's current over and under temperature sets incline matching the decline of the 'ideal' set (5). Instead, this will be modified such that it inclines towards a more 'extreme' temperature, which we'll define as being 10°C beyond the end of the ideal set (6).

Finalizing this change, the rules needed to be altered. First, the rule governing the neutral state when in the ideal set is removed. Instead, the output will be allowed to return to zero as discovered in testing. (9)

4.3.3 If no charge rules fire, the charge current defaults to 180kW

The output charge rate is determined by the rules that fire. If no rules hinting at an output charge are activated, the expectation is that the system will not output any charge - however, Output 1 defaults to the center of it's range, instead of 0.

This could theoretically by fixed by adding and refining a new rule to hint to no charging, but this adds complexity to the system, and increases the inference time. Instead, an easier solution is to widen the lower boundary of the range on the output to -360, such that 0 falls in the center of the output's range - effectively re-defining the default value. Note that the memberships on the output are not altered, thus the behaviour should otherwise be identical.

Implementing this change appears to have the exact effect desired, the output now has double the range, making the rule viewer graph smaller and a little harder to view, but in exchange for zero output current exactly as desired.(14)

4.3.4 Minor fault has opposite effect

During testing, it was observed that output current would rise when the minor fault was high, and fall when it was low; The precise compliment to the desired behaviour. Examining the rule base uncovered a mistake whilst implementing the rule base, where instead of the 'High' set (Set 2), the low set (Set 1) was accidentally selected; The mistake likely arising over confusion between counting the index from 0, rather than 1. Rectifying this simple mistake rectified this issue.

5 Conclusions

Whilst the system functions moderately well in the patterns it follows to meet NEC regulations for charging based on state of the battery, alongside regulating the temperature, it's become clear that the implementation is not accurate. Output values are not sufficiently limited, and often provide charging far exceeding appropriate levels for the current state of the inputs as suggested by the research. As provided, the product of this work cannot be used in the industry due to it's poor performance. The goal for this system was to prolong the lifetime of an electric vehicle by conditioning it's battery whilst charging. However, as it stands, the system would likely the exact opposite effect. It fails to meet the researched ideal values, as discussed in 4.1 output values for charging tend to remain high, and if tested in a working environment can be expected to exacerbate the degradation of the battery.

Further, there remains issues which would prevent the system from being considered suitable, such as the rules for High and Low temperatures alongside the rule for the minor fault which suggest that the output current should be lowered rather significantly in the name of safety or battery preservation. In the implementation, these rules have very little effect on the overall value of output 1.

Significant further work in issue correction and i/o calibration of the system would be required in order to iterate it to a state where it could have the potential of being production ready, however this prototype does indeed prove that there is indeed potential for fuzzy logic to be used this way in an EV charge system.

Appendices

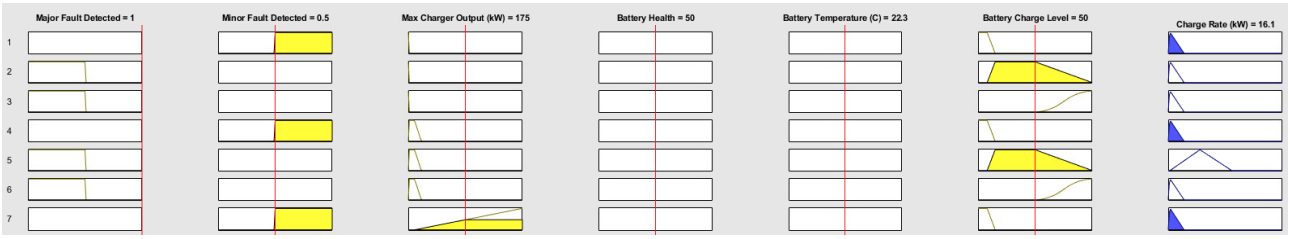

Figure 1: Current rules activating during a major fault.

```
bat_cl_low_1  =  [0, 2, 2, 0, 0, 1, 3, 0, 1, 2];
bat_cl_low_2  =  [0, 2, 3, 0, 0, 1, 3, 0, 1, 2];
bat_cl_low_3  =  [0, 2, 4, 0, 0, 1, 3, 0, 1, 2];

% Charge level
% Limits
bat_cl_low_1  =  [1, 0, 2, 0, 0, 1, 3, 0, 1, 1];
bat_cl_low_2  =  [1, 0, 3, 0, 0, 1, 3, 0, 1, 1];
bat_cl_low_3  =  [1, 0, 4, 0, 0, 1, 3, 0, 1, 1];

bat_cl_low_1_fault  =  [1, 2, 0, 0, 0, 1, 3, 0, 1, 1];
bat_cl_low_2_fault  =  [1, 2, 0, 0, 0, 1, 3, 0, 1, 1];
bat_cl_low_3_fault  =  [1, 2, 0, 0, 0, 1, 3, 0, 1, 1];
```

Figure 2: Current rules before and after splitting into separate rules.

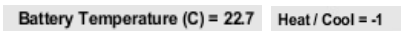

Figure 3: Call for cooling whilst at ideal temperature

```
bat_temp_low_temp       = [0, 0, 0, 0, 1, 0, 0, 3, 0.5, 1];
bat_temp_ideal_temp     = [0, 0, 0, 0, 2, 0, 0, 2, 1, 1];
bat_temp_high_temp      = [0, 0, 0, 0, 3, 0, 0, 1, 1, 1];

bat_temp_low_charge     = [1, 0, 0, 0, 1, 0, 3, 0, 0.5, 1];
% bat_temp_ideal_charge = [1, 0, 0, 0, 2, 0, 0, 0, 1, 1];
bat_temp_high_charge    = [1, 0, 0, 0, 3, 0, 3, 0, 1, 1];

bat_cl_low_1  =  [0, 2, 2, 0, 0, 1, 3, 0, 1, 2];
bat_cl_low_2  =  [0, 2, 3, 0, 0, 1, 3, 0, 1, 2];
bat_cl_low_3  =  [0, 2, 4, 0, 0, 1, 3, 0, 1, 2];

bat_cl_mid_1  =  [1, 0, 2, 0, 0, 2, 3, 0, 1, 1];
bat_cl_mid_2  =  [1, 0, 3, 0, 0, 2, 4, 0, 1, 1];
bat_cl_mid_3  =  [1, 0, 4, 0, 0, 2, 5, 0, 1, 1];

bat_cl_high_1 =  [1, 0, 2, 0, 0, 3, 3, 0, 1, 1];
bat_cl_high_2 =  [1, 0, 3, 0, 0, 3, 3, 0, 1, 1];
bat_cl_high_3 =  [1, 0, 4, 0, 0, 3, 3, 0, 1, 1];
limit_fault = [0 ,1 ,0 ,0 , 0, 1, 0, 1, 1]

% Charging current
limit_supply_L1 = [1, 0, 1, 0, 0, 0, 1, 0, 1, 1]
limit_supply_L2 = [1, 0, 2, 0, 0, 0, 2, 0, 1, 1]
limit_supply_L3 = [1, 0, 3, 0, 0, 0, 2, 0, 1, 1]
```

```
ruleList = [
    bat_cl_low_1;
    bat_cl_mid_1;
    bat_cl_high_1;
    bat_cl_low_2;
    bat_cl_mid_2;
    bat_cl_high_2;
    bat_cl_low_3;
    bat_cl_mid_3;
    bat_cl_high_3;
    bat_temp_low_charge;
%   bat_temp_ideal_charge;
    bat_temp_high_charge;
    bat_temp_low_temp;
    bat_temp_ideal_temp;
    bat_temp_high_temp;
    limit_fault;
    limit_supply_L1;
    limit_supply_L2;
    limit_supply_L3
    ];
```

Figure 4: The preliminary rulebase

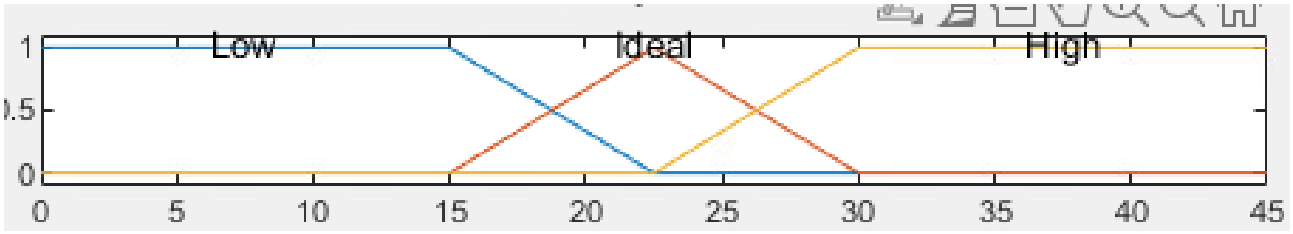

Figure 5: Input 5 before overhaul

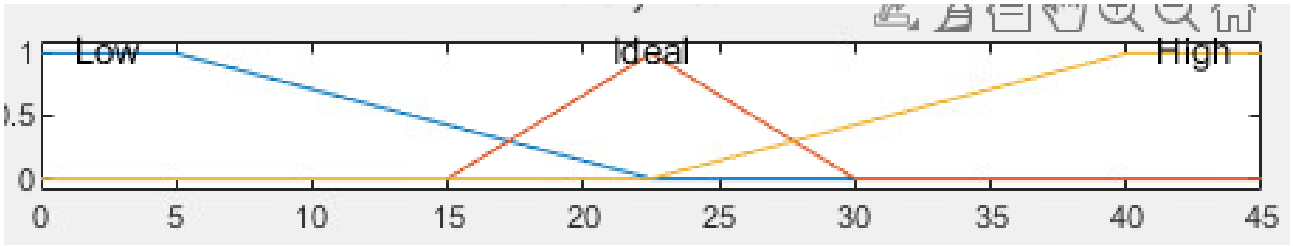

Figure 6: Input 5 after overhaul

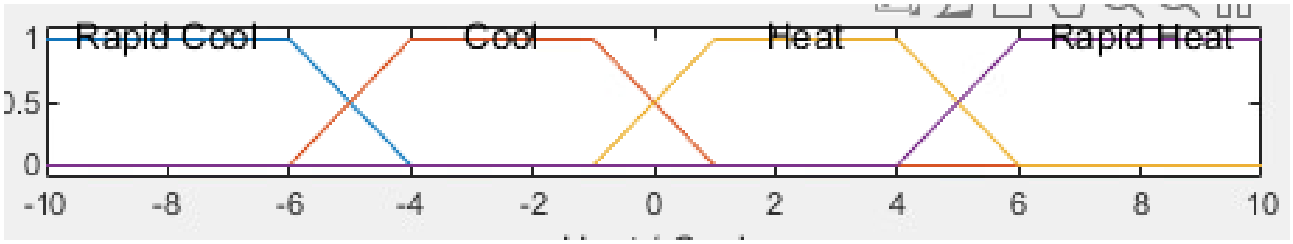


```
% Populating the output variable with membership functions
a = addmf(a, 'output', 2, 'Rapid Cool', 'trapmf',[-10 -10 -6 -4]);
a = addmf(a, 'output', 2, 'Cool',       'trapmf',[-6 -4 -1 1]);
a = addmf(a, 'output', 2, 'Heat',       'trapmf',[-1 1 4 6]);
a = addmf(a, 'output', 2, 'Rapid Heat', 'trapmf',[4 6 10 10]);
```

Figure 7: Output 2 before overhaul

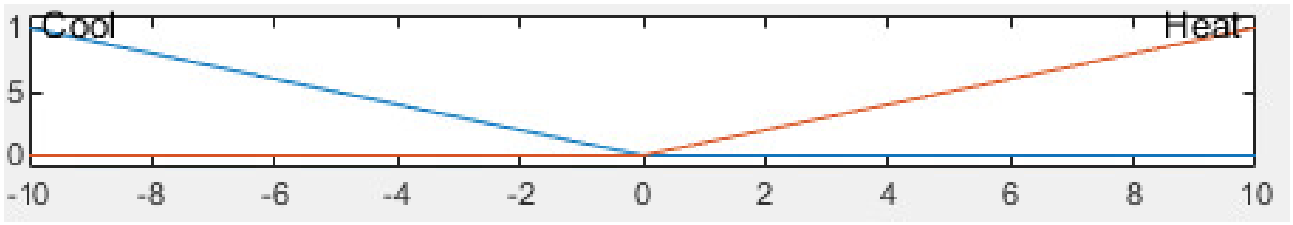


```
% Populating the output variable with membership functions
a = addmf(a, 'output', 2, 'Cool',       'trapmf',[-10 -10 -10 0]);
a = addmf(a, 'output', 2, 'Heat',       'trapmf',[0 10 10 10]);
```

Figure 8: Output 2 after overhaul

```
bat_temp_low_temp       = [0, 0, 0, 0, 1, 0, 0, 3, 0.5, 1];
bat_temp_ideal_temp     = [0, 0, 0, 0, 2, 0, 0, 2, 1, 1];
bat_temp_high_temp      = [0, 0, 0, 0, 3, 0, 0, 1, 1, 1];
bat_temp_low_temp       = [0, 0, 0, 0, 1, 0, 0, 3, 0.5, 1];
bat_temp_ideal_temp     = [0, 0, 0, 0, 2, 0, 0, 2, 1, 1];
bat_temp_high_temp      = [0, 0, 0, 0, 3, 0, 0, 1, 1, 1];
```

Figure 9: Temperature rules before and after overhaul

```
a = addmf(a, 'output', 2, 'Cool',       'zmf',[-10 0]);
a = addmf(a, 'output', 2, 'Heat',       'zmf',[0 10]);
```

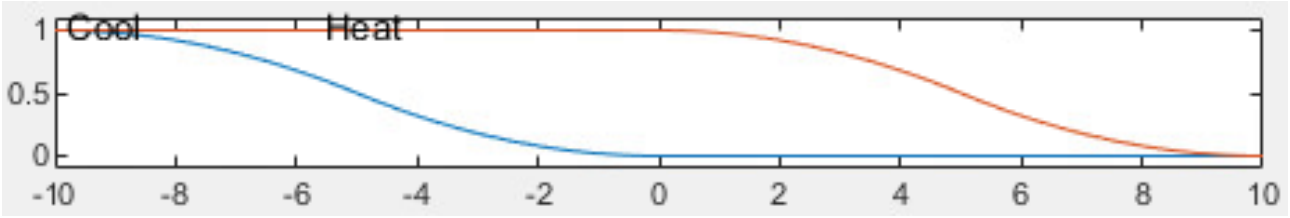


```
% Populating the output variable with membership functions
a = addmf(a, 'output', 2, 'Cool',       'trapmf',[-10 -10 -10 0]);
a = addmf(a, 'output', 2, 'Heat',       'trapmf',[0 10 10 10]);
```

Figure 10: A zmf definition, and it's output not matching what was expected - followed by the final implementation drawn using a trapmf

Major Fault	Minor Fault	Battery Health	Charger Max Output	Battery Charge Level	Battery Temperature
1	0	50	9	10	10
1	0	50	9	25	10
1	0	50	9	40	10
1	0	50	9	80	10
1	0	50	9	100	10
1	0	50	9	10	22.7
1	0	50	9	25	22.7
1	0	50	9	40	22.7
1	0	50	9	80	22.7
1	0	50	9	100	22.7
1	0	50	9	10	40
1	0	50	9	25	40
1	0	50	9	40	40
1	0	50	9	80	40
1	0	50	9	100	40
1	0	50	20	10	10
1	0	50	20	25	10
1	0	50	20	40	10
1	0	50	20	80	10
1	0	50	20	100	10
1	0	50	20	10	22.7
1	0	50	20	25	22.7
1	0	50	20	40	22.7
1	0	50	20	80	22.7
1	0	50	20	100	22.7
1	0	50	20	10	40
1	0	50	20	25	40
1	0	50	20	40	40
1	0	50	20	80	40
1	0	50	20	100	40
1	0	50	50	10	10
1	0	50	50	25	10
1	0	50	50	40	10
1	0	50	50	80	10
1	0	50	50	100	10
1	0	50	50	10	22.7
1	0	50	50	25	22.7
1	0	50	50	40	22.7
1	0	50	50	80	22.7
1	0	50	50	100	22.7
1	0	50	50	10	40
1	0	50	50	25	40
1	0	50	50	40	40
1	0	50	50	80	40
1	0	50	50	100	40
1	0	50	250	10	10
1	0	50	250	25	10
1	0	50	250	40	10
1	0	50	250	80	10
1	0	50	250	100	10
1	0	50	250	10	22.7
1	0	50	250	25	22.7
1	0	50	250	40	22.7
1	0	50	250	80	22.7
1	0	50	250	100	22.7
1	0	50	250	10	40
1	0	50	250	25	40
1	0	50	250	40	40

Figure 11: The test data used as the base for most tests.

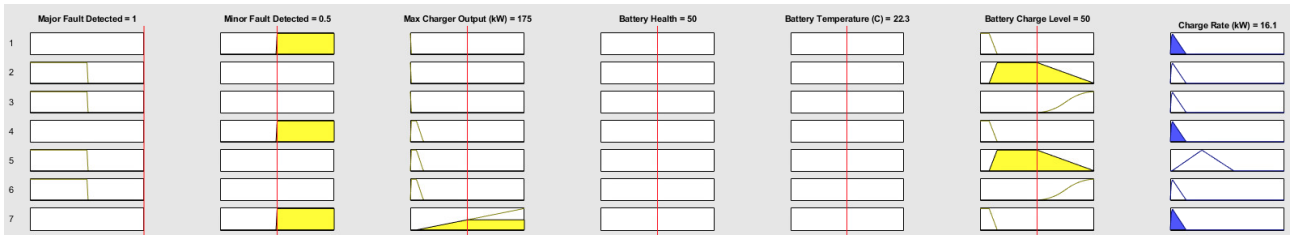

Figure 12: Rules firing, delivering current when no current was expected.

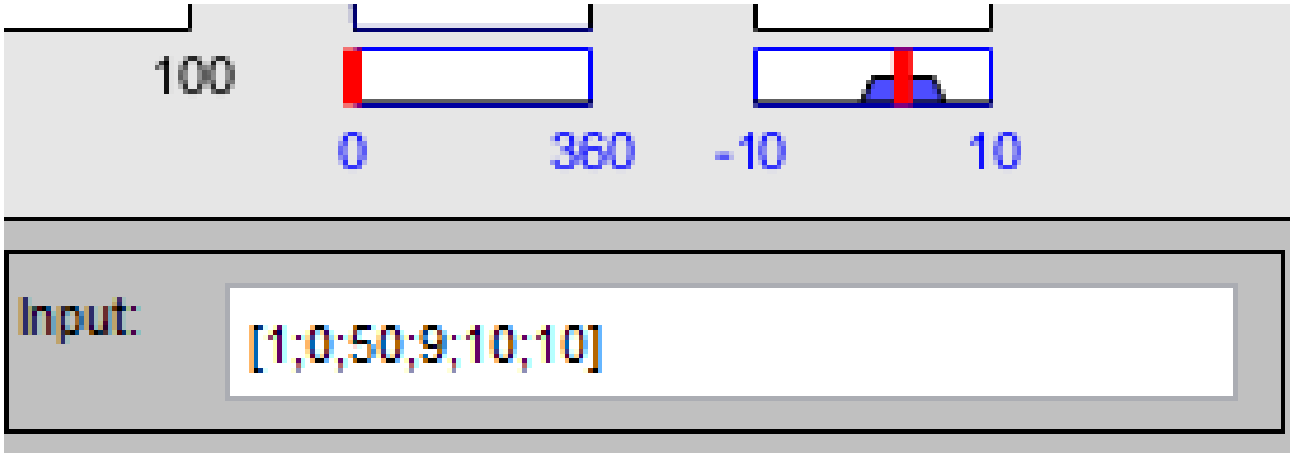

Figure 13: Manually entering data from the failed test shows a passing result.

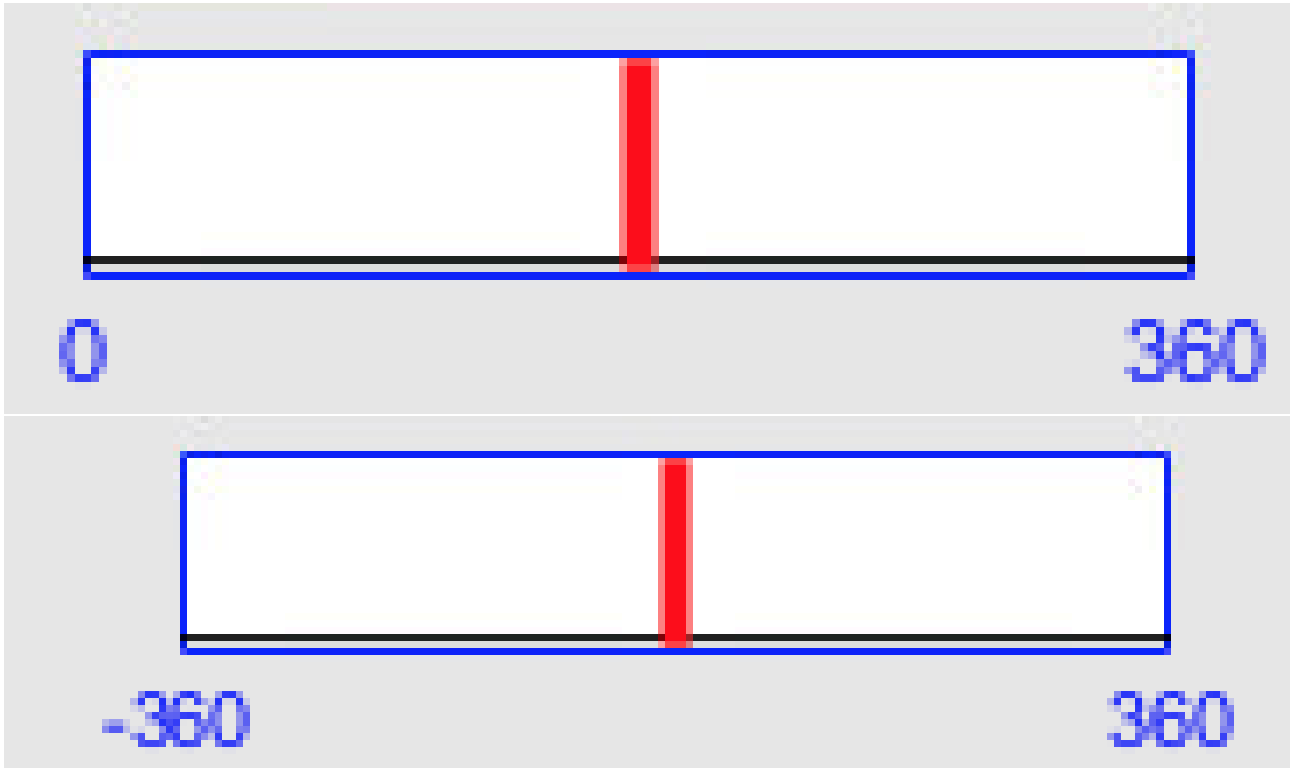

Figure 14: Output 1 after altering the lower boundary.

```
bat_cl_low_1  =  [1, 0, 2, 0, 0, 1, 3, 0, 1, 1];
bat_cl_low_2  =  [1, 0, 3, 0, 0, 1, 3, 0, 1, 1];
bat_cl_low_3  =  [1, 0, 4, 0, 0, 1, 3, 0, 1, 1];

bat_cl_mid_1  =  [1, 0, 2, 0, 0, 2, 3, 0, 1, 1];
bat_cl_mid_2  =  [1, 0, 3, 0, 0, 2, 4, 0, 1, 1];
bat_cl_mid_3  =  [1, 0, 4, 0, 0, 2, 5, 0, 1, 1];

bat_cl_high_1 =  [1, 0, 2, 0, 0, 3, 3, 0, 1, 1];
bat_cl_high_2 =  [1, 0, 3, 0, 0, 3, 3, 0, 1, 1];
bat_cl_high_3 =  [1, 0, 4, 0, 0, 3, 3, 0, 1, 1];
```

Figure 15: The temperature management rules

Centroid		Bisector		lom		mom		som	
73.35	6.51	64.80	6.80	0.00	10.00	0.00	8.60	0.00	7.20
85.10	6.51	93.60	6.80	0.00	10.00	0.00	8.60	0.00	7.20
85.10	6.51	93.60	6.80	0.00	10.00	0.00	8.60	0.00	7.20
78.38	6.51	72.00	6.80	0.00	10.00	0.00	8.60	0.00	7.20
14.74	6.51	14.40	6.80	0.00	10.00	0.00	8.60	0.00	7.20
73.35	-5.10	64.80	-5.20	0.00	-10.00	0.00	-5.10	0.00	-0.20
94.96	-5.10	100.80	-5.20	0.00	-10.00	0.00	-5.10	0.00	-0.20
94.96	-5.10	100.80	-5.20	0.00	-10.00	0.00	-5.10	0.00	-0.20
78.78	-5.10	72.00	-5.20	0.00	-10.00	0.00	-5.10	0.00	-0.20
14.74	-5.10	14.40	-5.20	0.00	-10.00	0.00	-5.10	0.00	-0.20
71.08	-6.73	57.60	-7.20	0.00	-10.00	0.00	-10.00	0.00	-10.00
83.51	-6.73	86.40	-7.20	0.00	-10.00	0.00	-10.00	0.00	-10.00
83.51	-6.73	86.40	-7.20	0.00	-10.00	0.00	-10.00	0.00	-10.00
76.35	-6.73	72.00	-7.20	0.00	-10.00	0.00	-10.00	0.00	-10.00
14.74	-6.73	14.40	-7.20	0.00	-10.00	0.00	-10.00	0.00	-10.00
74.83	6.51	64.80	6.80	0.00	10.00	0.00	8.60	0.00	7.20
85.93	6.51	93.60	6.80	100.80	10.00	50.40	8.60	0.00	7.20
85.93	6.51	93.60	6.80	100.80	10.00	50.40	8.60	0.00	7.20
79.61	6.51	79.20	6.80	0.00	10.00	0.00	8.60	0.00	7.20
14.89	6.51	14.40	6.80	7.20	10.00	3.60	8.60	0.00	7.20
74.83	-5.10	64.80	-5.20	0.00	-10.00	0.00	-5.10	0.00	-0.20
95.92	-5.10	100.80	-5.20	100.80	-10.00	50.40	-5.10	0.00	-0.20
95.92	-5.10	100.80	-5.20	100.80	-10.00	50.40	-5.10	0.00	-0.20
80.01	-5.10	79.20	-5.20	0.00	-10.00	0.00	-5.10	0.00	-0.20
14.89	-5.10	14.40	-5.20	7.20	-10.00	3.60	-5.10	0.00	-0.20
72.52	-6.73	57.60	-7.20	7.20	-10.00	7.20	-10.00	7.20	-10.00
84.32	-6.73	86.40	-7.20	7.20	-10.00	7.20	-10.00	7.20	-10.00
84.32	-6.73	86.40	-7.20	7.20	-10.00	7.20	-10.00	7.20	-10.00
77.54	-6.73	72.00	-7.20	7.20	-10.00	7.20	-10.00	7.20	-10.00
14.87	-6.73	14.40	-7.20	7.20	-10.00	7.20	-10.00	7.20	-10.00
132.55	6.51	36.00	6.80	14.40	10.00	10.80	8.60	7.20	7.20
132.55	6.51	36.00	6.80	14.40	10.00	10.80	8.60	7.20	7.20
132.55	6.51	36.00	6.80	14.40	10.00	10.80	8.60	7.20	7.20
132.55	6.51	36.00	6.80	14.40	10.00	10.80	8.60	7.20	7.20
20.27	6.51	21.60	6.80	14.40	10.00	10.80	8.60	7.20	7.20
220.29	-5.10	237.60	-5.20	360.00	-10.00	222.55	-5.10	7.20	-0.20
255.67	-5.10	259.20	-5.20	360.00	-10.00	266.40	-5.10	172.80	-0.20
255.67	-5.10	259.20	-5.20	360.00	-10.00	266.40	-5.10	172.80	-0.20
220.29	-5.10	237.60	-5.20	360.00	-10.00	222.55	-5.10	7.20	-0.20
25.20	-5.10	21.60	-5.20	43.20	-10.00	25.20	-5.10	7.20	-0.20
125.31	-6.73	36.00	-7.20	7.20	-10.00	7.20	-10.00	7.20	-10.00
125.31	-6.73	36.00	-7.20	7.20	-10.00	7.20	-10.00	7.20	-10.00
125.31	-6.73	36.00	-7.20	7.20	-10.00	7.20	-10.00	7.20	-10.00
125.31	-6.73	36.00	-7.20	7.20	-10.00	7.20	-10.00	7.20	-10.00
19.10	-6.73	14.40	-7.20	7.20	-10.00	7.20	-10.00	7.20	-10.00
197.36	6.51	230.40	6.80	14.40	10.00	10.80	8.60	7.20	7.20
238.45	6.51	273.60	6.80	14.40	10.00	10.80	8.60	7.20	7.20
238.45	6.51	273.60	6.80	14.40	10.00	10.80	8.60	7.20	7.20
214.40	6.51	252.00	6.80	14.40	10.00	10.80	8.60	7.20	7.20
20.27	6.51	21.60	6.80	14.40	10.00	10.80	8.60	7.20	7.20
197.96	-5.10	237.60	-5.20	14.40	-10.00	10.80	-5.10	7.20	-0.20
285.73	-5.10	295.20	-5.20	360.00	-10.00	331.20	-5.10	302.40	-0.20
285.73	-5.10	295.20	-5.20	360.00	-10.00	331.20	-5.10	302.40	-0.20
215.52	-5.10	252.00	-5.20	14.40	-10.00	10.80	-5.10	7.20	-0.20
20.37	-5.10	21.60	-5.20	14.40	-10.00	10.80	-5.10	7.20	-0.20
191.13	-6.73	230.40	-7.20	7.20	-10.00	7.20	-10.00	7.20	-10.00
233.68	-6.73	273.60	-7.20	7.20	-10.00	7.20	-10.00	7.20	-10.00
233.68	-6.73	273.60	-7.20	7.20	-10.00	7.20	-10.00	7.20	-10.00
208.79	-6.73	244.80	-7.20	7.20	-10.00	7.20	-10.00	7.20	-10.00
19.10	-6.73	14.40	-7.20	7.20	-10.00	7.20	-10.00	7.20	-10.00

Figure 16: The evaluation results provided by the system after testing with 11

Distance from max				
64.35	55.80	9.00	9.00	9.00
76.10	84.60	9.00	9.00	9.00
76.10	84.60	9.00	9.00	9.00
69.38	63.00	9.00	9.00	9.00
5.74	5.40	9.00	9.00	9.00
64.35	55.80	9.00	9.00	9.00
85.96	91.80	9.00	9.00	9.00
85.96	91.80	9.00	9.00	9.00
69.78	63.00	9.00	9.00	9.00
5.74	5.40	9.00	9.00	9.00
62.08	48.60	9.00	9.00	9.00
74.51	77.40	9.00	9.00	9.00
74.51	77.40	9.00	9.00	9.00
67.35	63.00	9.00	9.00	9.00
5.74	5.40	9.00	9.00	9.00
54.83	44.80	20.00	20.00	20.00
65.93	73.60	80.80	30.40	20.00
65.93	73.60	80.80	30.40	20.00
59.61	59.20	20.00	20.00	20.00
5.11	5.60	12.80	16.40	20.00
54.83	44.80	20.00	20.00	20.00
75.92	80.80	80.80	30.40	20.00
75.92	80.80	80.80	30.40	20.00
60.01	59.20	20.00	20.00	20.00
5.11	5.60	12.80	16.40	20.00
52.52	37.60	12.80	12.80	12.80
64.32	66.40	12.80	12.80	12.80
64.32	66.40	12.80	12.80	12.80
57.54	52.00	12.80	12.80	12.80
5.13	5.60	12.80	12.80	12.80
82.55	14.00	35.60	39.20	42.80
82.55	14.00	35.60	39.20	42.80
82.55	14.00	35.60	39.20	42.80
82.55	14.00	35.60	39.20	42.80
29.73	28.40	35.60	39.20	42.80
170.29	187.60	310.00	172.55	42.80
205.67	209.20	310.00	216.40	122.80
205.67	209.20	310.00	216.40	122.80
170.29	187.60	310.00	172.55	42.80
24.80	28.40	6.80	24.80	42.80
75.31	14.00	42.80	42.80	42.80
75.31	14.00	42.80	42.80	42.80
75.31	14.00	42.80	42.80	42.80
75.31	14.00	42.80	42.80	42.80
30.90	35.60	42.80	42.80	42.80
52.64	19.60	235.60	239.20	242.80
11.55	23.60	235.60	239.20	242.80
11.55	23.60	235.60	239.20	242.80
35.60	2.00	235.60	239.20	242.80
229.73	228.40	235.60	239.20	242.80
52.04	12.40	235.60	239.20	242.80
35.73	45.20	110.00	81.20	52.40
35.73	45.20	110.00	81.20	52.40
34.48	2.00	235.60	239.20	242.80
229.63	228.40	235.60	239.20	242.80
58.87	19.60	242.80	242.80	242.80
16.32	23.60	242.80	242.80	242.80
16.32	23.60	242.80	242.80	242.80
41.21	5.20	242.80	242.80	242.80
230.90	235.60	242.80	242.80	242.80

Figure 17: How far away the values in 16 were from the maximum charging current available.

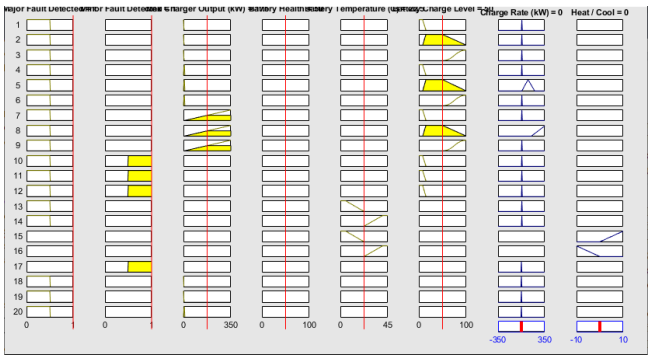

Figure 18: No output being provided when major and minor and high.

References

(2007).
URL: *https://home.howstuffworks.com/home-thermostat.htm*

(2017).
URL: *https://www.tesla.com/en*$_G$*B/support/vehicle − warranty*

Agwu, D. D., Opara, F., Chukwuchekwa, N., Dike, D. & Uzoechi, L. (2018), 'Review of comparative battery energy storage systems (bess) for energy storage applications in tropical enviroments'.

Bower, G. (2015), 'Electric vehicle charging levels explained'.
URL: *https://insideevs.com/news/328781/electric-vehicle-charging-levels-explained/*

Database, E. (2021), 'Tesla model 3 performance'.
URL: *https://ev-database.uk/car/1322/Tesla-Model-3-Performance*

David, G. (2009), 'Keep an eye on temperature trends during li-ion battery charge and discharge cycles'.
URL: *https://www.electronicdesign.com/technologies/boards/article/21749397/keep-an-eye-on-temperature-trends-during-liion-battery-charge-and-discharge-cycles*

Dober (2020), 'Electric vehicle cooling systems'.
URL: *https://www.dober.com/electric-vehicle-cooling-systems*

Electric Vehicle Charging Equipment Installation Guide (2020).
URL: *https://web.archive.org/web/20000902051830/http://www.state.ma.us/doer/programs/ev/charge*

Karnik, N. N. & Mendel, J. M. (2001), 'Centroid of a type-2 fuzzy set', *Information Sciences* **132**(1–4), 195–220.
URL: *https://linkinghub.elsevier.com/retrieve/pii/S002002550100069X*

Khan, A. B. & Choi, W. (2018), 'Optimal charge pattern for the high-performance multi-stage constant current charge method for the li-ion batteries', *IEEE Transactions on Energy Conversion* **33**(3), 1132–1140.

Lambert, F. (2020), 'A look at tesla battery degradation and replacement after 400,000 miles'.
URL: *https://electrek.co/2020/06/06/tesla-battery-degradation-replacement/*

LIANG, Y. C. & NG, T. K. (1993), 'Design of battery charging system with fuzzy logic controller', *International Journal of Electronics* **75**(1), 75–86.
URL: *https://doi.org/10.1080/00207219308907089*

Lilly, C. (2021), 'Electric car market statistics', *Next Green Car - Green car guide* .
URL: *https://www.nextgreencar.com/electric-cars/statistics*

Mamdani, E. & Assilian, S. (1975), 'An experiment in linguistic synthesis with a fuzzy logic controller', *International Journal of Man-Machine Studies* **7**(1), 1–13.
URL: *https://linkinghub.elsevier.com/retrieve/pii/S0020737375800022*

Mathwords (2021), 'Defuzzification methods'.
URL: *https://www.mathworks.com/help/fuzzy/defuzzification-methods.html*

Mendel, J., Hagras, H., Tan, W.-W., Melek, W. W. & Ying, H. (2014), *Introduction To Type-2 Fuzzy Logic Control: Theory and Applications*, John Wiley Sons. Google-Books-ID: C1HcAwAAQBAJ.

Novak, V., Perfilieva, I. & Mockor, J. (1999), *Mathematical principles of fuzzy logic*, Kluwer international series in engineering and computer science, Kluwer Academic.

Oh, H. & Park, S. (2014), 'Effect of coolant flow characteristics in cooling plates on the performance of hev/ev battery cooling systems', *Transactions of the Korean Society of Automotive Engineers* **22**(3), 179–185.
URL: *https://www.koreascience.or.kr/article/JAKO201411560023063.page*

Ouyang, D., Weng, J., Chen, M., Liu, J. & Wang, J. (2020), 'Experimental analysis on the degradation behavior of overdischarged lithium-ion battery combined with the effect of high-temperature environment', *International Journal of Energy Research* **44**(1), 229–241.
URL: *https://onlinelibrary.wiley.com/doi/abs/10.1002/er.4898*

Ouyang, D., Weng, J., Liu, J., Chen, M. & Wang, J. (2019), 'Influence of current rate on the degradation behavior of lithium-ion battery under overcharge condition', *Journal of The Electrochemical Society* **166**(12), A2697–A2706.
URL: *https://doi.org/10.1149/2.1441912jes*

Smith, K., Shi, Y. & Santhanagopalan, S. (2015), Degradation mechanisms and lifetime prediction for lithium-ion batteries — a control perspective, *in* '2015 American Control Conference (ACC)', p. 728–730.

Thomson, M. T. (1999), 'Nec 1999 art. 625'.
URL: *http://www.madkatz.com/ev/nec1999Article625.html*

Valle, B., Wentz, C. & Sarpeshkar, R. (2011), 'An area and power-efficient analog li-ion battery charger circuit', *IEEE transactions on biomedical circuits and systems* **5**, 131–137.

Walton, B., Hamilton, J., Alberts, G., Fullerton-Smith, S., Day, E. & Ringrow, J. (2020), 'Electric vehicles - setting a course for 2030', *Deloitte Insights* .
URL: *https://www2.deloitte.com/us/en/insights/focus/future-of-mobility/electric-vehicle-trends-2030.html*

Wang, Q., Jiang, B., Xue, Q. F., Sun, H. L., Li, B., Zou, H. M. & Yan, Y. Y. (2015), 'Experimental investigation on ev battery cooling and heating by heat pipes', *Applied Thermal Engineering* **88**, 54–60.
URL: *https://www.sciencedirect.com/science/article/pii/S1359431114008679*